High-Frequency Ground Motion Simulation Using a Source- and Site-Specific Empirical Green's Function Approach

R. Mourhatch & S. Krishnan
California Institute of Technology, Pasadena, CA, USA

SUMMARY:
A key limitation of seismic wave propagation simulations is that the seismic wave-speed structure of the earth is not well resolved for propagating high-frequency waves. The high frequencies in the ground motion must be simulated through other means. Toward this end, we adopt the classical empirical Green's function (EGF) approach of summing recorded seismograms from past small earthquakes with suitable time-shifts to generate seismograms for large events. Whereas, in the past, the magnitude of events used as EGFs were limited to within 1 or 2 units of the target event's magnitude, this source- and site-specific approach allows us to use vast number of seismograms from very small earthquakes (magnitudes 2.5-3.5) as EGFs to produce the high-frequency content of large earthquakes. We are expanding the envelope of the empirical Green's functions approach by using large number of seismograms from small earthquakes as EGFs to produce high frequency content of large earthquakes.

Keywords: Empirical Green's Function, High Frequency Ground Motions

1. INTRODUCTION

The purpose of this work is to produce site-specific broadband ground motions in southern California from a suite of large earthquakes on the San Andreas fault. A major challenge in seismology is predicting the expected ground motions from large earthquakes for future events. These predictions are essential for hazard estimation, engineering design, and risk analysis.

Theoretically, to produce site-specific ground motions deterministically, one needs detailed description of: (1) the earthquake source mechanism and (2) wave-speed structure of the travel path. The frequency content of the ground motions generated using deterministic finite/spectral-element or finite difference approaches is limited by our knowledge and resolution of those aspects. The knowledge about earthquake source process is limited by many factors arising mainly from our lack of understanding about various source model parameters and their relations to one another; however reasonable assumptions can be made based on the best available information collected from past earthquakes. The resolution of the seismic wave-speed structure is a key governing factor in determining the limits of the frequency content of the propagating waves (the higher the resolution of the velocity structure the higher the frequency content). This resolution is limited by the spatial density of seismic observations, which is relatively low when compared to the size of the region. Even in the most well studied regions (such as southern California) the wave-speed models (i.e. CVM-H 11.9) are capable of propagating waves with frequencies up to 0.5 Hz (in some recent studies up to 1 Hz), well below that required for many engineering applications. To overcome this limitation, hybrid approaches are used that combine the long period shaking histories from a deterministic simulation and the high-frequency shaking histories from a stochastic approach, typically using Green's functions representing the response measured at a station due to a unit impulse at the seismic source.

We are using such a hybrid approach for generating ground motions from large earthquakes. The low

frequency content (<0.5 Hz) of the ground motion is generated deterministically using a spectral element based program called SPECFEM3D, which incorporates the regional wave-speed structure in three dimensions. The low frequency content from such a deterministic simulation is then superposed with high-frequency shaking generated using source- and site-specific EGF approach, which will be the main focus of this article.

Hartzell (1978) first introduced the concept of empirical Green's function (EGF) method; he proposed using aftershock records of an event as the Green's functions (EGFs) to capture the travel path of the seismic wave. Since then, several variations of the method have been proposed by many scholars [e.g., Irikura (1983), Joyner and Boore (1986), Heaton and Hartzell (1989), Somerville (1991), Tumarkin et al. (1994) and Frankel (1995)]. In these methods, the rupture plane of the target event is subdivided into a typically uniform grid of subfaults and the shaking from all the subfaults is time-shifted and summed to yield the shaking under the target event.

An inherent problem with the EGF method is the incoherent scaling of the high- or low-frequency content and inconsistencies with Brune's spectral scaling law (Brune (1970)). At one extreme, one can add the events such that the moment of the target event equals the total moment of all added events (in the simplest case of using one EGF this can be viewed as scaling based on the seismic moment of the EGF to that of the target event), this produces the correct low frequency content (below the corner frequency of the large event) and overestimates the high frequency content (above the corner frequency of the small event). On the other hand, one can fill the rupture area with non-overlapping events (scaling based on area, which is equivalent to scaling based on moment ratios to the power of 2/3), which tends to reproduce high frequency content accurately (above the corner frequency of the small event) with deficiencies in low frequencies. Joyner and Boore (1986) were one of the earliest to recognize this problem. They suggested a summation scheme that matched Brune's spectral scaling law. In that work it was suggested that $N^{4/3}$ events be randomly added in time over the total rise time of the event and the final result be multiplied by $N^{-1/3}$ (N is the ratio of the seismic moment of the main event to the seismic moment of the EGF). Heaton and Hartzell (1989) also presented a quantitative discussion on the source of inconsistency in the use of EGFs. To generate broadband ground motion, other works have proposed filtering either the EGFs or the final results to match the observed coherency in high and low frequencies. For example, some scholars have suggested adding enough events to match the moment and convolving each added record with stochastic source time functions to reduce the high frequency content without modulating the low frequencies. Others have suggested populating the rupture area with non-overlapping events and then applying appropriate filers (designed based on relative slip velocities of the target event and the small event) to increase the low frequency content without modulating the high frequency content (Frankel 1995, Somerville 1991).

Here, we are using the EGF approach to produce only the high frequency (0.5-10 Hz) part of the ground motions to be combined with the low frequency part from wave propagation simulations. We start with kinematic source models from past earthquakes resampled to a 0.5 by 0.5 km resolution; the choice of this resolution is dictated by the maximum frequency content that our deterministic approach is capable of reliably producing as dictated by the resolution of the wave-speed model. We select EGFs from historical recorded events in the 2.5-3.5 magnitude range located in the vicinity of the target event. The main assumption here is that the source mechanism of the small event is the same as that of the target event. Our formulation consists of two summations, one over all the subfaults and one within each subfault. In both summations proper time shifts are applied to account for rupture front propagation. In the second summation, the EGFs are further shifted in time to ensure that the "impulse" source-time functions of the EGFs collectively approximate the source-time functions of the target sub-event associated with the subfault. Additional correction is applied to the records to correct for geometric spreading. The key advances in this work are, expanding the limits of applicability of the EGF method by utilizing the large quantity of the seismic data available in the low magnitude range and subtle variation in the summing procedure, which eliminates the need for filtration or convolution (for matching the Brune's spectrum) within the frequency band of interest. We validate our approach by simulating the 2004 Parkfield (M_w 6.0), 1999 Hector Mine (M_w 7.1) and 2010 Baja California (M_w 7.2) earthquakes at various stations across southern California.

2. METHODOLOGY

The algorithm for producing the high frequency ground motions consists of three major tasks: (1) source model selection and modification, (2) EGF event selection and quality check, and (3) EGF summation. To eliminate the lower frequencies, the synthetics are filtered using a high-pass Butterworth filter with its corner frequency at 0.5 Hz. The high frequency waveforms are then superimposed on top of low frequency ground motion waveforms that are generated using SPECFEM3D to synthesize broad band ground motion histories (up to 10 Hz).

2.1. High Frequency Ground Motions

2.1.1 Source Model Selection & Modification

The source models are selected from kinematic finite source inversions of past earthquakes on faults that are geometrically similar to that of the target event, with a rupture mechanism similar to that of the target event. For example, for simulating a San Andreas fault event, the source models will be limited to past earthquakes that happened on faults with a dip angle of approximately 90^{o} and a maximum depth of 20 km. Furthermore their rupture mechanisms should be close to right lateral strike slip, the rupture mechanisms historically observed on the San Andreas fault. The assumption here is that the properties of the earthquakes will be similar if the fault geometry and mechanism are similar.

After selecting the proper source model, the source model is resampled to 0.5 km by 0.5 km subfault resolution (if the provided resolution is coarser than 0.5 km by 0.5 km). This resolution is obtained based on the rupture front propagation and the limiting frequency content of the deterministic approach (see section 2.2). Fig. 2.1. illustrates the source model for the 2004 Parkfield earthquake [Source modeller: Dr. Chen Ji (UCSB)].

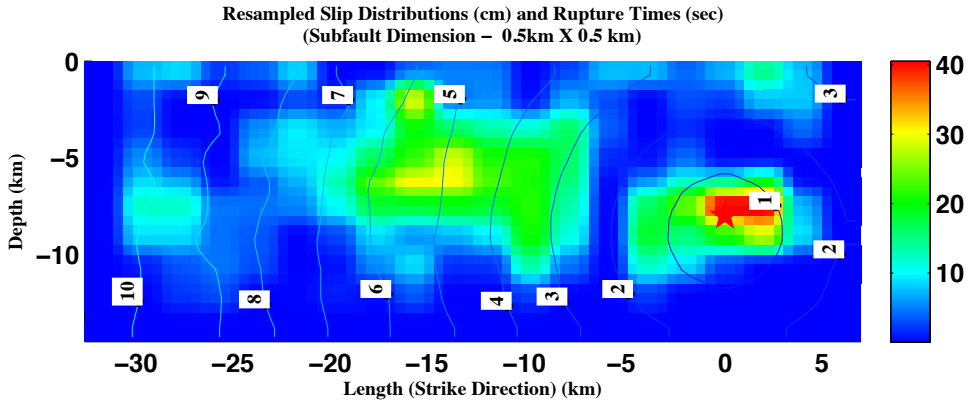

Figure 2.1. Resampled inverted source model for 2004 M_w 6.0 Parkfield earthquake [Dr. Chen Ji (UCSB)]. Color map: slip distribution in centimetres | Counter lines: rupture times | Star: hypocenter of the event

2.1.2. EGF Event Selection

For each subfault we select a record, from a set of small earthquakes, that best matches the target subfault-target station's path. Each record is then checked to satisfy a pre-specified signal-to-noise ratio and overall quality factor. A schematic representation of EGF event election is shown in Fig. 2.2. of all the historical records available in the vicinity of the i^{th} station from earthquakes on the fault located in the vicinity of the j^{th} subfault, the record "g_{ij}" best represents the path between the i^{th} station and the j^{th} subfault (Irikura 1983).

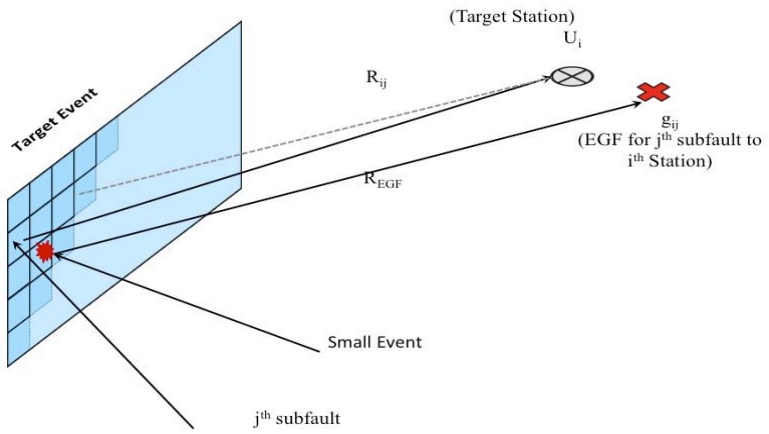

Figure 2.2. Schematic for event selection

2.1.3. Summation

The summation procedure involves two summations, one over all subfaults and one within each subfault (Eqn. 2.1). In the first summation, the EGF assigned for each subfault (g_{ij}) is shifted in time by the amount of time it takes for the rupture-front to arrive at the j^{th} subfault (t_{rup}^{J}). Additionally, each record is scaled by the ratio of distances from the subfault to the target station R_{ij} and from the EGF hypocenter to the EGF station R_{EGF} (see Fig. 2.2) to account for the differences in geometric spreading between the real EGF's path and the target's path.

In the second summation (summation within each subfault) the corrected records for each subfault are summed such that the total seismic moment of the summed records is equal to the seismic moment of the subfault. The number of records needed K_j is estimated by the ratio of the seismic moment of the subfault to that of the EGF, rounded down to the nearest integer. Since the records are rounded down, there is an additional correction involving moments (second parentheses in Eqn. 2.1), which needs to be applied in order to account for discrepancies arising from adding an integer amount of EGFs. In the second summation, the records are shifted within the rise time of the subfault based on the functional form of the source sampling function $f_j(k)$, which is derived from the shape of the source time function of the subfault source time function associated with source model of the target event. Fig. 2.3 (d) illustrates the functional form of $f_i(k)$ for a triangular source time function. In general, this function can be considered as the discrete form of the source time function. In previous studies, in order to match the source time function, $f_i(k)$ was estimated by dividing the rise time into K_j equal time shifts and introducing Dirac delta functions uniformly at distances equal to this time shift. However, we use a different functional form for f(k), which is based on equal moment release over time [horizontal divisions in Fig. 2.3. (c)]. Our source time function approximation matches the total amount of seismic moment, however it accomplishes this with an uneven distribution of Dirac delta functions in time. This ensures a smoother moment release during the middle half duration of the rise time, which reduces the high frequency content to a great extent.

$$U_i(x,t) = \sum_{j=1}^{N} \sum_{k=1}^{K_j} \left(\frac{R_{ij}}{R_{EGF}} \right) \left(\frac{M_{o^j}}{K_j M_{o^{EGF}}} \right) g_{ij}[x, t - t_{rup^j} - f_j(k)] \tag{2.1}$$

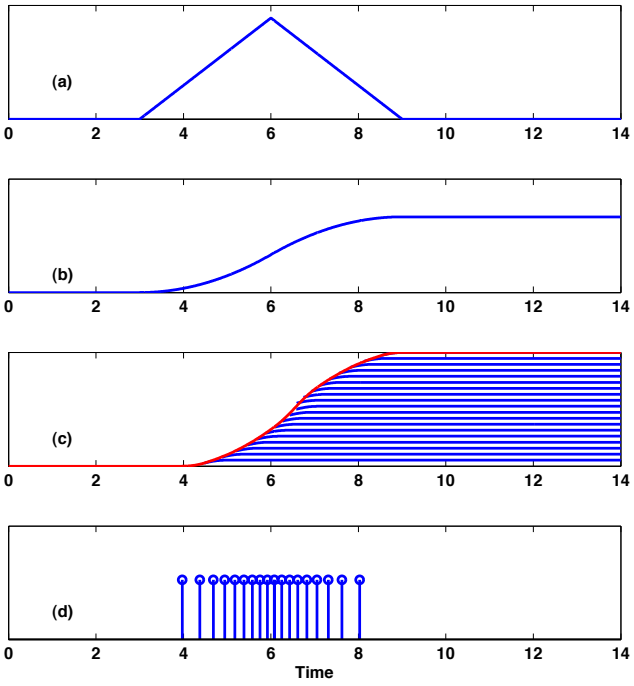

Figure 2.3. f (k) Estimation. (a) Moment rate (or slip rate) vs. time | (b) moment (or slip) vs. time (integral of (a) | (c) Approximation of (b) using multiple EGFs | (d) f (k): Delta functions representing time shifts needed to generate the approximation in (c)

2.2. Low Frequency Content

The low frequency ground motion waveforms are generated using the spectral-element based program SPECFEM3D-SESAME. For southern California, we use the SCEC CVM-H 11.9 wave-speed model, through which we can reliably propagate seismic waves with frequencies up to 0.5 Hz (down to 2 sec period). Additionally, to generate the shortest wave in this range, a burst of at least five impulses must occur within the spatial extent of one wave-length. Based on rupture propagation speed and the wave-speed model of the earth, the source models should be resampled to a maximum of 0.5 by 0.5 km subfault to be capable of generating this frequency content.

3. RESULTS

We simulate three earthquakes here to validate the approach: (1) 2004 M_w 6.0 Parkfield earthquake (2) 1999 M_w 7.1 Hector Mine earthquake, and (3) 2010 M_w 7.2 Baja California earthquake. For each event, we select at least 40 broadband records from sites at various distances ranging from roughly 15 km to 350 km. The EGF records were obtained from the Southern California Earthquake Data Center (SCEDC) Seismogram Transfer Program (STP). At the current stage, the metric for our comparisons of the results are the velocity time series and the spectral amplitude of the velocity time series.

Fig. 3.1. illustrates the location of all the stations used in the Parkfield validation. The resampled source model is shown in Fig. 2.1. Fault strike is 137^o, fault dip is 83^o, and rupture area is 40 km in the strike direction and 14.5 km in the dip direction. The original subfault dimensions is 2 km in the strike and 1.45 km in the dip direction. Single triangular function is used as the source time function for the individual subfaults. High-frequency ground motions are produced using small earthquakes in the 2.5-3.5-magnitude range.

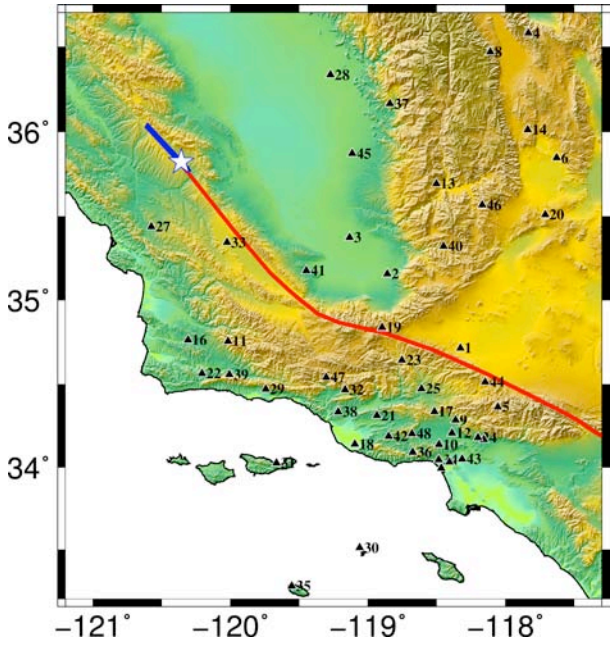

Figure 3.1. Location of all stations used in validation of the Parkfield earthquake. Red line: San Andreas Fault | Blue line: surface trace of 2004 Parkfield earthquake surface trace | Star: 2004 Parkfield earthquake hypocenter | Black triangles: stations |

Fig. 3.2 shows the high frequency ground motion for north-south (N-S) and east-west (E-W) components of velocity time series at the site of station 1, located at roughly 250 km south-west of the 2004 Parkfield earthquake hypocenter. The records shown in black are the actual Parkfield record and the records shown in red are the simulated records. Fig. 3.3 illustrates the low frequency ground motion contents for the same station (N-S, E-W) generated using SPECFEM3D. The superimposed ground motions for the same station are illustrated in Fig. 3.4. The velocity spectra of the synthetics are being compared in Fig 3.5.

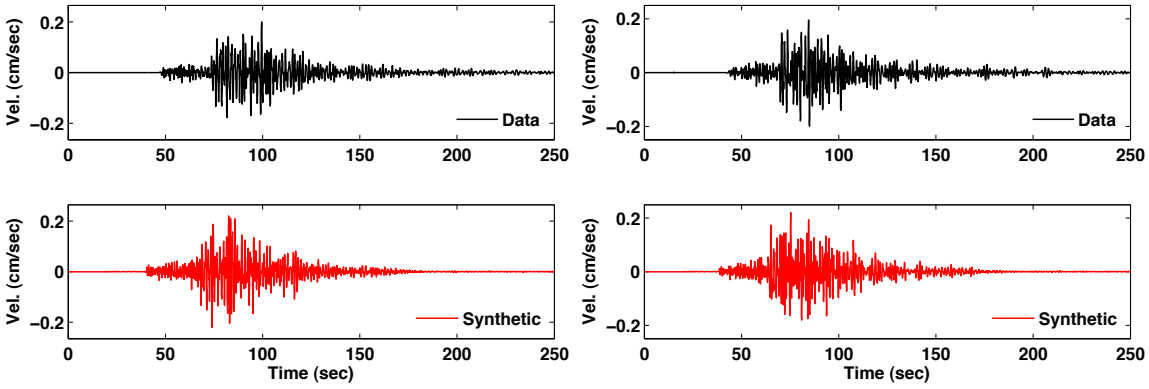

Figure 3.2. Comparisons of high frequency (0.5-10 Hz) ground motions at station 1 | Left column: North-South component | Right column: East-West component | Top row: observed ground motions | Bottom row: Synthetic ground motions

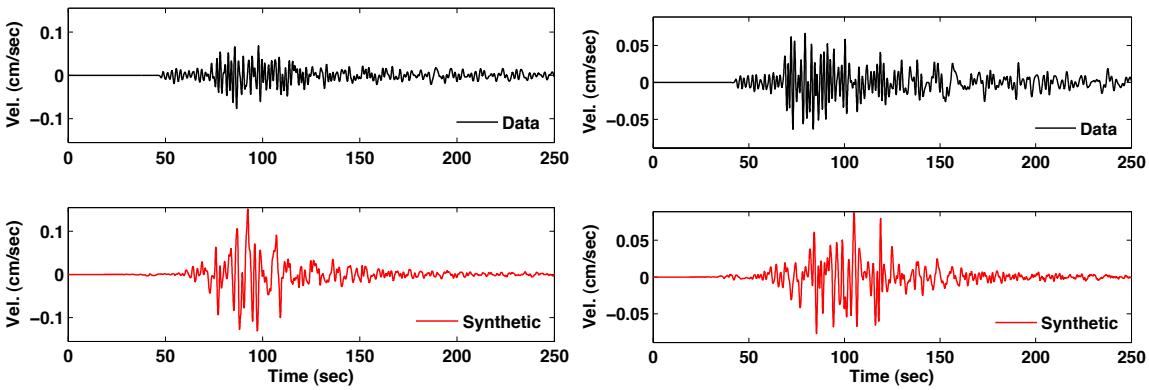

Figure 3.3. Comparisons low frequency (< 0.5 Hz) ground motions at station 1 | Left column: North-South component | Right column: East-West component | Top row: observed ground motions | Bottom row: Synthetic ground motions

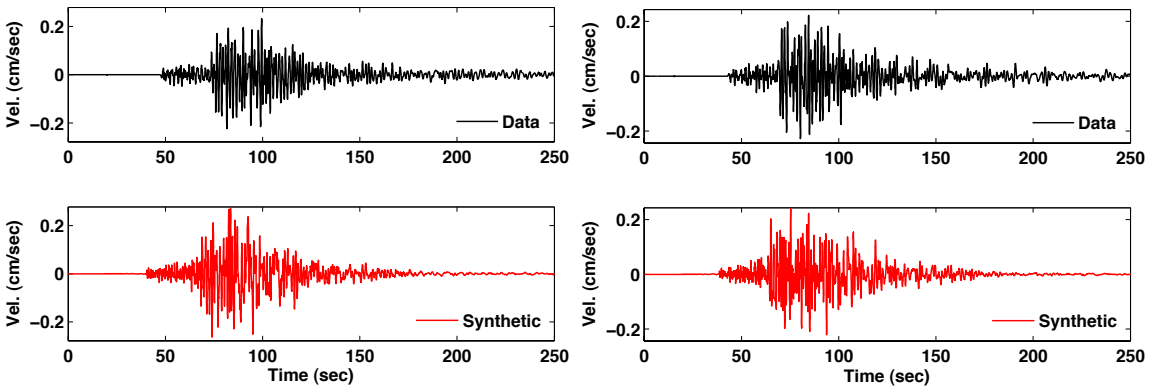

Figure 3.4. Comparisons of broadband ground motions at station 1 | Left column: North-South component | Right column: East-West component | Top row: observed ground motions | Bottom row: Synthetic ground motions

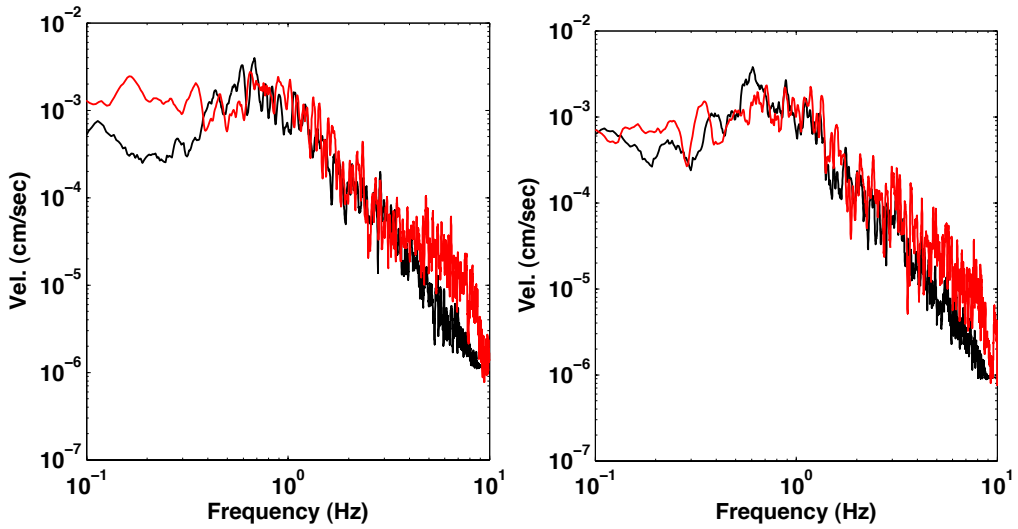

Figure 3.5. Comparison of velocity spectras | Left column: North-South component | Right column: East-West component | Black: observed ground motions | Red: synthetic ground motions

The figures show a good agreement between the observed and simulated results. The overall shape of the envelope of the time domain synthetics (peak values, location of the peak values and the duration

of the records for high frequencies) shows good agreement between the simulated and observed results. Additionally, the agreement between the spectra of the velocities shows promising results without significant overestimations or underestimations at any particular frequency range. The results are more encouraging considering the magnitude of the EGFs and the distance of the station to the hypocenter of the earthquake. The success in these preliminary results show that the use of source- and site-specific low magnitude EGFs in conjunction with kinematic source models from past earthquakes, with an emphasis on matching and creating smooth source time functions can result in realistic ground motion simulations suitable for various engineering applications.

5. FUTURE WORK

While the preliminary results are encouraging, a full statistical analysis of the results is necessary to establish the robustness of this method. Currently, we are performing quantitative statistical comparisons between real data and synthetics. We are planning to examine the influence of source models developed by different modelers, and the effect of various source parameters on our results. Furthermore, we will be investigating the relation between the quality of the results and the magnitudes of EGFs at various distances.

AKCNOWLEDGEMENT

We thank Chen Ji (UCSB) and Martin Mai (KAUST) for providing source models from past earthquakes, Dimitri Komatitsch (University of Pau, France) for insights into SPECFEM3D, Carl Tape (UAF) for providing the wave-speed model for SPECFEM3D, Thomas Heaton (Caltech) and Robert Graves (USGS Pasadena) for their insights into the Empirical Green's Function method and ground motion simulations.

We gratefully acknowledge the funding provided by the National Science Foundation (NSF Award No. 0926962)

REFERENCES

Brune, J. N. (1970). Tectonic stress and the spectra of seismic shear waves from earthquakes. *Journal of Geophysical Research*. **75:26**, 4997-5009

Frankel, A. (1995). Simulating strong motions of large earthquakes using recordings of small earthquakes: The Loma Prieta mainshock as a test case. *Bulletin of the Seismological Society of America.* **85**, 1144-1160

Hartzell, S.H. (1978). Earthquake aftershocks as Green's functions. *Geophysical Research Letters*. **5:1**, 1-4

Heaton, T.H., and Hartzell, S.H. (1989). Estimation of strong ground motions from hypothetical earthquakes on Cascadia subduction zone, Pacific Northwest. *Pure and Applied Geophysics.* **129:1/2.** 131-201

Irikura, K. (1983). Semi-empirical estimation of strong ground motions during large eartquakes. *Bull. Disas. Prev. Res. Inst. Kyoto Univ.* **33:2**, 63-104

Ji, C., Wald, D.J. and Helmberger, D.V. (2002). Source description of the 1999 Hector Mine, California earthquake; Part I: Wavelet domain inversion theory and resolution analysis, *Bulletin of the Seismological Society of America.* **92:4**, 1192-1207

Joyner, W. B. and Boore, D. M. (1986). On simulating large earthquakes by Green's function addition of small earthquakes. *Proceddings of the 5th Maurice Ewing Symposium on earthquake source mechanics.*

Sommerville, P. Sen, M. Cohee, B. (1991). Simulation of strong ground motions recorded during the 1985 Michoacan, Mexico, and Valparaiso, Chile, earthquakes. *Bulletin of the Seismological Society of America.* **81**, 1-27

Tumarkin, A.G. Archuleta, R.J. Madariaga, R. (1994). Scaling relations of composite earthquake models. *Bulletin of the Seismological Society of America.* **84:4**, 1279-1283